Advanced Materials Research *Online: 2013-07-15*
ISSN: 1662-8985, Vol. 717, pp 37-43
doi:10.4028/www.scientific.net/AMR.717.37

A New Synthesis of $BaHPO_4$ Precipitated by $BaCO_3$-H_3PO_4-NaOH System at Room Temperature

Banjong Boonchom[1,3,a], Chesta Ruttanapun[2,3,b], Montree Thongkam[1,3,c], Pachernchaipat Chaiyasith[1,3,d], Somsak Woramongkonchai[1,3,e], Samart Kongteweelert[1, 3, f], and Naratip Vittayakorn[1, 4,5,6, g],

[1]Department of Chemistry, Faculty of Science, King Mongkut's Institute of Technology Ladkrabang, Ladkrabang, Bangkok, 10520, Thailand

[2]Department of Physcis, Faculty of Science, King Mongkut's Institute of Technology Ladkrabang, Ladkrabang, Bangkok, 10520, Thailand

[3]Functional Phosphate Materials and Alternative Fuel Energies Research Unit (FPM-AFE), King Mongkut's Institute of Technology Ladkrabang, Ladkrabang, Bangkok, 10520, Thailand

[4] Electroceramic Research Laboratory, College of KMITL Nanotechnology, King Mongkut's Institute of Technology Ladkrabang, Bangkok 10520, Thailand

[5]ThEP Center, CHE, 328 Si Ayutthaya Rd., Bangkok 10400, Thailand

[6]Advanced Materials Science Research Unit, Department of Chemistry, Faculty of Science, King Mongkut's Institute of Technology Ladkrabang, Bangkok 10520, Thailand

[a,] *kbbanjon@gmail.com, [b]chesta.ruttanapun@gmail.com, [c]mjacky27@hotmail.com, [d]pachemchaiput@gmail.com, [e]kwsomsa@kmitl.ac.th, [f]samart75@hotmail.com,Naratipcmu@yahoo.com

Keywords: Characterization inorganic phosphate compounds; New synthesis; Non-uniform and porous structure ; Thermodynamic properties

Abstract. Barium hydrogenphosphate, $BaHPO_4$ was synthesized for the first time through simple and rapid method using $BaCO_3$-H_3PO_4-NaOH, pH =9.0 at room temperature for 30 min. The studied $BaHPO_4$ decomposed in a single well-defined stage via deprotonated hydrogenphosphate reactions, revealed by TG/DTG and DSC techniques. The calculated wavenumbers based on DSC peak were comparable with FTIR results, which support the breaking bonds of P-OH (HPO_4^{2-}) in the deprotonated hydrogenphosphate reactions. The thermodynamic functions (ΔH^*, ΔG^*, and ΔS^*) for the deprotonated hydrogenphosphate reactions calculated from DSC data indicate that the deprotonated HPO_4^{2-} reaction occur a lower-energy pathway and spontaneous process. The FTIR, XRD and SEM data of the studied $BaHPO_4$ and its decomposed product $Ba_2P_2O_7$ are also reported.

Introduction

Inorganic phosphate compounds contain a large class of diverse materials whose application includes: catalysis, ion exchange, proton conductivity, food additive, fertilizer, detergent, fuel cell, intercalation chemistry, photochemistry, pigment, surface coating, bond and teeth [1-5]. They have attracted more and more interests on synthesis, crystallography, electro-optical material, morphology and so on [5–10]. Among inorganic phosphate compounds, alkaline earth phosphates such as $MHPO_4$ (M = Mg, Ca, Sr, Ba) have been extensively studied in the past years for their applications in different domains such as bioceramics, ionic conductivity, bone, teeth, pigment and luminescence [11-18].

For interesting compound, $BaHPO_4$ have been widely investigated due to their proper crystal structures and utilizations [11-19]. There were many studies on the crystal structures of $BaHPO_4$, which have two forms as α-$BaHPO_4$ and β-$BaHPO_4$ and crystallize on orthorhombic system [16, 18]. Vibrational studies of α- or β-$BaHPO_4$ were published [14, 16, 18]. Thermal transformation of $BaHPO_4$ to $Ba_2P_2O_7$ was proposed in the literatures [12, 18]. The decomposed mechanisms were different depend on the obtained $BaHPO_4$ by synthetic routes. But there were a few papers about the synthetic methods of barium hydrogenphosphate that determine the properties of material. So far, $BaHPO_4$ was synthesized from precipitation method using different starting raw materials: H_3PO_4-

$Ba(OH)_2$-$NH_3 \cdot H_2O$ at room temperature for 3 hrs [13], H_3PO_4-$BaCl_2 \cdot 2H_2O$-$C_6H_{15}N$-NaCl at 180 ^oC for 5 days[16], H_3PO_4-$Ba(OH)_2$ at 100 ^oC for 2 days[18], and NaH_2PO_4-$BaCl_2$- poly(ethylene glycol) acrylate-copoly(methacrylic acid) (PEGA-PMAA) at room temperature for 1 day[17].

The ambition of this work was to synthesize $BaHPO_4$ by precipitation route using $BaCO_3$-H_3PO_4-NaOH at room temperature for 30 min, which is a simple and cost-effective route. Thermal transformation of $BaHPO_4$ to $Ba_2P_2O_7$ was observed by thermogravimetric analysis (TG/DTG) and differential scanning calorimetry (DSC). The crystal structure, vibrational study, and non-uniform and porous structure will be also discussed. Some details in this work were reported for the first time such as a new raw material ($BaCO_3$) and room temperature with short time consuming for synthesis, thermodynamic functions, the calculated wavenumbers from thermal data of thermal transformation, and the obtained particle shape.

Experimental

Barium hydrogen phosphate, $BaHPO_4$ compound was prepared by precipitation method using $BaCO_3$ (>99% purity, Merck), phosphoric acid (86.4%w/w H_3PO_4, Merck) and NaOH (99.8%, Carlo Erba) as starting materials. The synthesis of $BaHPO_4$ was made according to eq.1

$$BaCO_3(s) + H_3PO_4(aq) \xrightarrow{\text{NaOH, pH = 9.0}} BaHPO_4(s) + H_2O(l) + CO_2(g) \quad (1)$$

In a successful synthesis run to yield $BaHPO_4$, 3.0 g of barium carbonate ($BaCO_3$) were dissolved by 13 mL of 1 M phosphoric acid (H_3PO_4) in a beaker and then was magnetically stirred at room temperature until the colourless solution was obtained. Then, 1 M NaOH was added into the solution for adjusting pH =9.0 and the white precipitates were completely obtained for 30 min. The obtained white powders were recovered by vacuum filtration and air drying.

Thermogravimetry (TG) and derivative thermogravimetry (DTG) data were carried out by a Perkin Elmer, TGA Pyris 1. The powder sample (6.00 mg) was heated in alumina crucible against an alumina reference under nitrogen (N_2) flow rate of 100 mL min^{-1} starting from room temperature up to 800 ^oC at a heating rate of 10 ^oC min^{-1}.

Differential Scanning Calorimetry (DSC) curves was studied by a Perkin-Elmer DSC 204 F1 Phoenix apparatus over a temperature range from 50 to 600 ^oC under flowing argon at a flow of 50 mL min^{-1}. Nearly 6 mg of sample was taken in the Pt crucible and experiments were carried out at the heating rates of 10 ^oC min^{-1}.

The specificity of the thermal decomposition was characterized by identification of the bonds to be selectively activated due to energy absorption at vibrational level [19, 20]. These breaking bonds were assigned and compared with the observed wavenumbers in the IR spectra. The relation between the T_p on DSC curve and the wavenumbers of the activated bond is given as follows:

$$\omega = \frac{k_b}{hc} T_P = 0.695 T_p \quad (2)$$

where k_b and h are respectively the Boltzmann and Planck constants, and c the light velocity. Because the breaking bond has an unharmonic behavior, the specific activation is possible also due to more than one quanta, or by a higher harmonic: $\omega_{sp} = q\omega_{calc}$, $q \in N$, where ω_{sp} is the assigned spectroscopic number for the bond supposed to break.

The structure and crystallite sizes of the prepared sample and its decomposed product were studied by X-ray powder diffraction using a D8 Advanced powder diffractometer (Bruker AXS, Karlsruhe, Germany) with Cu K_α radiation (λ = 0.1546 nm). The Scherrer method was used to evaluate the crystalline size [21].

The room temperature FTIR spectra were recorded in the range of 4000-400 cm^{-1} with eight scans on a Perkin-Elmer Spectrum GX spectrometer with the resolution of 4 cm^{-1}. The samples were thoroughly mixed with dried KBr (approx. 1 parts sample : 200 parts KBr).

Powder morphologies and particle size were figured directly using a scanning electron microscope (SEM, LEO1455 VP) after gold coating.

Results and discussion

The synthesized $BaHPO_4$ powders were successfully obtained by a simple route using a new raw material ($BaCO_3$) and room temperature with short time period (30 min.). The percentage yield was 90 %.

The TG-DTG curves of $BaHPO_4$ in nitrogen (N_2) atmosphere are shown in Fig.1. The TG curve shows the mass losses in the range of room temperature and 800 °C, which are related to an intramolecular dehydration of the deprotonated hydrogenphosphate groups. The thermal transformation formally could be presented as:

$$BaHPO_4(s) \longrightarrow 1/2Ba_2P_2O_7(s) + 1/2H_2O(g) \quad (3)$$

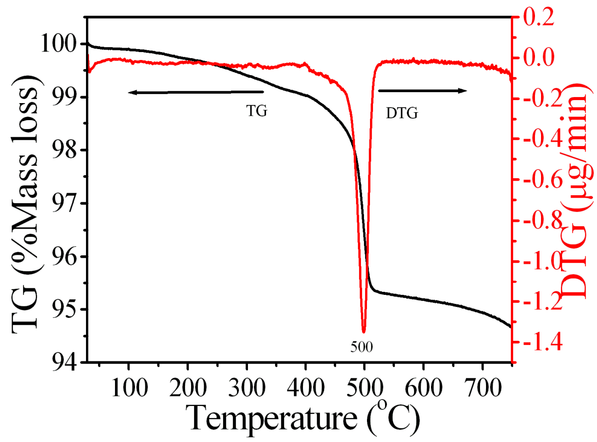

Fig.1 TG/DTG curves of $BaHPO_4$ in N_2 at a heating rate of 10 K min^{-1}

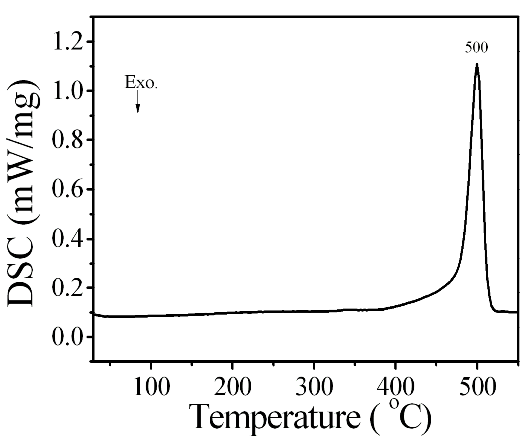

Fig.2 DSC curves of $BaHPO_4$ in N_2 at a heating rate of 10 K min^{-1}

TG trace shows the mass losses in area of 300-550 °C corresponding to mass losses of 4.53%, which is close to the theoretical value (3.86 %). A single well-defined stage shown on TG curve respected to a DTG peak and a endothermic DSC peak (Fig. 2) (500 °C). In order to gain the complete decomposition of synthesized $BaHPO_4$ in air atmosphere, the sample of $BaHPO_4$ was heated in a furnace at 600 °C for 2 h and thermal transformation product was found to be $Ba_2P_2O_7$. The thermal transformation temperature of $BaHPO_4$ to $Ba_2P_2O_7$ obtained by $BaCO_3$-H_3PO_4-NaOH system in this work (500 °C) is higher than that obtained by $BaCl_2$•$2H_2O$-H_3PO_4-$C_6H_{15}N$-NaCl system reported by BenChaabane et. al.(415 °C) [16]. Additionally, thermal transformation mechanism of $BaHPO_4$ reported in this work (a single step) is different from that of $BaHPO_4$ reported in previous work (more than one step) [18]. The result clearly indicates that the thermal behaviors of materials could be depended on synthetic method as well as condition reaction; raw materials, media, pH, temperature and time consuming.

In order to corroborate the calculated data with the spectroscopic ones, we drew up the FT-IR spectrum of the studied $BaHPO_4$ compound. According to the above-mentioned equation (2), the T_p (DSC) for the single decomposition step is 500 °C. The calculated harmonic energy (ω_{calc}) values are 1074, 1611 and 3222 cm^{-1}, which correspond to 2, 3 and 6 quanta numbers, respectively. These wavenumbers are assigned to asymmetric phosphate mode ($\nu_3(F_2)PO_4^{3-}$), C band of HPO_4^{2-}, and A band of HPO_4^{2-}, which is close to the vibrational modes reported in the literature [19, 20]. These data confirm the breaking bonds of the true P–OH for the HPO_4^{2-} unit, which is referred to a continuous intermolecular polycondensation and then eliminated water molecule. The studied compound exhibited a very good agreement between the calculated wavenumbers from average T_p (DSC) and the observed wavenumbers from FT-IR spectrum for the bonds suggested being broken, which confirm the single thermal decomposition step according to eq. 3. The calculated wavenumbers from average T_p (DSC) using eq. 2 are convenience and simple method for the identification of the breaking bonds during the reaction, which are used for discussion about the decomposition steps.

The calculated values of ΔH*, ΔS* and ΔG* were calculated by DSC data (Fig.2) and found to be 3.96 kJ mol^{-1}, 0.01 J K^{-1} mol^{-1} and -0.42 kJ mol^{-1}, respectively. The enthalpy of activation (ΔH*) value for the decomposition step is positive that means that the reaction was endothermic process. The entropy of activation (ΔS*) value is positive. It means that its decomposed product was with lower degree of arrangement than the studied compound. Finally, the negative value of ΔG* shows that it is spontaneous process. These data indicate that the transformation of $BaHPO_4$ to $Ba_2P_2O_7$ can occur without the introduction of heat and a lower-energy pathway.

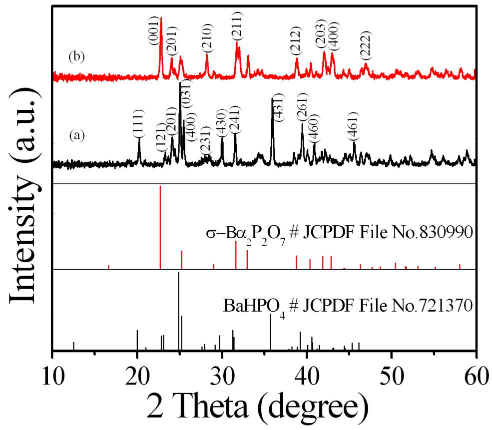

Fig.3 XRD patterns of $BaHPO_4$ (a) and its decomposition product $Ba_2P_2O_7$ (b)

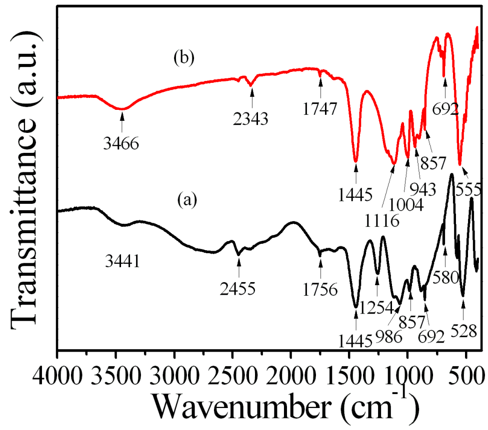

Fig.4 FTIR spectra of $BaHPO_4$ (a) and its decomposition product $Ba_2P_2O_7$(b)

The XRD patterns of the synthesized $BaHPO_4$ and its decomposed product $Ba_2P_2O_7$ are shown in Fig. 3. All detectable peaks of the obtained $BaHPO_4$ and $Ba_2P_2O_7$ samples are indexed as the standard data of JCPDF file no 721370 for $BaHPO_4$ and JCPDF file no 830990 for $Ba_2P_2O_7$, respectively. These results indicated that the $BaHPO_4$ crystal structure is in orthorhombic system with space group $Pn2_1a$ (33) (Z=12) and the $Ba_2P_2O_7$ crystal structure is in hexagonal system with space group P62m(189). The average crystallite size of 64 ± 12 nm for $BaHPO_4$ sample was calculated from X-ray line broadening of the reflections of (111), (031), (430), (241), and (431), using Scherrer equation (i.e. $D = 0.89\lambda/\beta\cos\theta$), where λ is the wavelength of X-ray radiation, D is a constant taken as 0.89, θ is the diffraction angle and β is the full width at half maximum (fwhm)[21]. Similarly, the average crystallite size of 52 ± 15 nm for the calcined sample ($Ba_2P_2O_7$) was calculated from X-ray line broadening of the reflections of (001), (201), (210), (211) and (400). The crystallite sizes and lattice parameters are also tabulated in Table 1. As it is shown Table 1, the lattice parameters of $BaHPO_4$ and $Ba_2P_2O_7$ are close to those of the standard data of JCPDF file no 721370 and JCPDF file no 830990, respectively.

The FT-IR spectra of $BaHPO_4$ and its decomposed product $Ba_2P_2O_7$ are shown in Fig. 4. The spectrum of $BaHPO_4$ illustrates the same characteristics as that of the fundamental vibrating unit, HPO_4^{2-} [14, 16, 18]. Vibrational bands of HPO_4^{2-} ion are observed in the regions of 300-3500 cm^{-1}. The formers consist in a number of distinct and well separated groups of bands. They may be regarded as being composed of the following frequency regions: the 380–600 cm^{-1} and the 800–1200 cm^{-1} range of PO_4^{3-} internal bending and stretching modes, respectively, and the high-frequency region 1200–3500 cm^{-1} corresponding to the hydrogen motions. Vibrational analysis for an isolated PO_4^{3-} anion with T_d point group leads to four normal modes: A_1(ν_1 mode), E (ν_2) and F_2 (ν_3 and ν_4) with average wavenumbers of 938, 420, 1017 and 567 cm^{-1}, respectively, [14, 16,18]. All of them are Raman active, whereas only ν_3 and ν_4 are IR active. In the $BaHPO_4$ crystal, the PO_4^{3-} ions occupy sites of lower symmetry than that of the free ion, anisotropic crystal fields may remove degeneracies and allow inactive mode to become active. Two very strong intensity bands at 986 and 998 cm^{-1} are indeed observed for different orientations and can be easily assigned to this non-degenerate mode. This result is in agreement with the presence of two crystallographically distinct PO_4 groups. The asymmetric stretching mode ν_3 appears in the 1000–1124 cm^{-1} region. This may be due either to overlapping or to accidental degeneracy. For the symmetric bending mode ν_2, only two corresponding bands are observed in the range 400–425 cm^{-1}. The asymmetric bending mode ν_4 is found in 500–590 cm^{-1} region with degeneracy strong bands. Typical vibrations of title compound is the appearance of the characteristic ABC structure of the ν(OH) vibration bands [14, 16,18] because of the existence of a variety of strongly hydrogen bonded solid. The problem of the origin of the *ABC* trio is discussed in many studies on acidic salts, but an explanation of this behavior of strongly hydrogen-bonded systems is still to be found [14, 16, 18]. One of the most popular interpretations of the *ABC* trio suggests a strong Fermi resonance between the ν(OH) stretching fundamentals and the overtones [2δ(OH) and 2γ(OH)] or combinations involving the δ(OH) and γ(OH) vibrations. Usually, the *ABC* bands are very broad and consist of many ill-resolved components. Two bands centered at 3200-2900 and 2550-2200 cm^{-1} in the FTIR spectrum are referred to as bands A and B, respectively. The third component (band C) is observed around 1800-1600 cm^{-1}. The typical intense bands at about 1254 cm^{-1} is due to the in plane P-O-H bending (A_2), while the out of plane bending (A_1) vibration is observed at about 857 cm^{-1}. The bands found between 3400 and 1350 cm^{-1} are assigned to overtone vibrations of the strong vibrations below 1300 cm^{-1}, the band located at 2690 $cm^{-1}$was assigned earlier to interionic Ba–O phonon bands [14, 16, 18].

The FTIR spectrum of the $BaHPO_4$ calcined at 600 ^{0}C (Fig.4) has been reported that the degree multiplication and fineness in the spectra of phosphates increase as the degree of polymerization increase in the tetrahedral $[PO_3]^{3-}$[10, 11]. It is clearly noticed that the studied compounds exhibit more splitting and sharpness, especially in the low-frequency region, indicating polymerization of $[PO_4^{3-}]$ to $[P_2O_7]^{4-}$. The strong vibration bands at 1116 and 1004 cm^{-1} are attributed to the stretching of PO_3 unit. The asymmetric (ν_{asym} POP) and symmetric stretch (ν_{sym} POP) bridge vibration for this sample are observed at about 943 and 857 cm^{-1}, while the asymmetric (δ_{asym} PO_3) and symmetric (δ_{sym} PO_3) bending vibration are observed at about 692and 555 cm^{-1}, respectively.

The SEM micrographs of $BaHPO_4$ and its decomposed product $Ba_2P_2O_7$ are shown in Fig.5. It clears that the shapes of the $BaHPO_4$ and $Ba_2P_2O_7$ appear non-uniform and porous structure, of which the pore sizes are about 1-10 mm. The morphology of $BaHPO_4$ shows smooth surface white that of $Ba_2P_2O_7$ appears roughness on the surface. The result is cause from the elimination of water in decomposition process. Although it seems that the particles have the tendency to congregate into clusters, the distribution is disordered (Fig. 5a and b). From the SEM images, we can see the crystal particles arrange from non-uniform and porous structure, via aggregate clusters, to small pore to large pore with uniform size. The mechanism of the whole changing process remains unclear and needs further study.

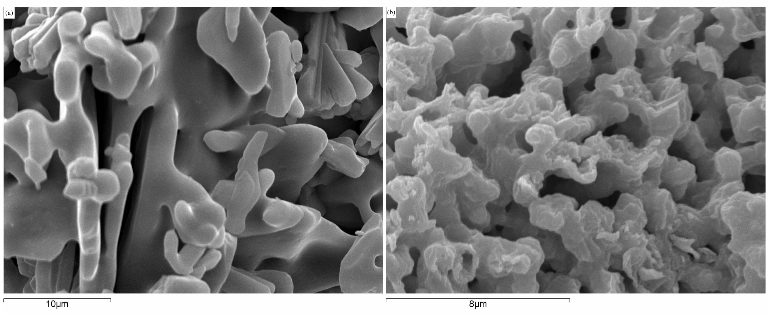

Fig.5 SEM micrograph of $BaHPO_4$ (a) and its decomposition product $Ba_2P_2O_7$ (b)

Conclusions

Barium hydrogen phosphate, $BaHPO_4$ was successfully precipitated by a new synthesis using $BaCO_3$-H_3PO_4-NaOH, pH=9 at room temperature with short time consuming (30 min). Thermal decomposition of $BaHPO_4$ to $Ba_2P_2O_7$ involves a single stage of the deprotonated hydrogenphosphate reaction, which is different from that of other works due to raw materials and conditions of preparations are the cause. The calculated wavenumber from thermal data assigned to the vibrational modes of the breaking bonds confirm the decomposition step. Thermodynamic data indicate that thermal transformation of $BaHPO_4$ to $Ba_2P_2O_7$ is occurred easy and spontaneous process. The prepared $BaHPO_4$ and $Ba_2P_2O_7$ products were confirmed by XRD and FTIR, which reveal crystal structure and fundamental vibration. SEM micrographs of $BaHPO_4$ and $Ba_2P_2O_7$ show diverse shapes and consist non-uniform and porous structure, via aggregate clusters, to small pore to large pore with uniform size. This obtained research displays that a new method is necessary for elaboration of technology and academic scientist to produce the $BaHPO_4$ and $Ba_2P_2O_7$, which play a large role in industrial applications.

Acknowledgement

The authors would like to acknowledge the financial support from development researcher grant through KMITL Research Fund (KREF#045504), King Mongkut't Institute of Technology Ladkrabang, Ministry of Education, Thailand.

References

[1] M.T. Averbuch-Pouchat, A.Durif, Topics in Phosphate Chemistry, first ed., World Scientific, Singapore 1996.

[2] P. Sundaramoorthi, G. Kanchana, S. Kalainathan, Spectrochemic Acta A. 69, (2008), pp. 1154–1159.

[3] S. Suri, K.K. Bamzai, V. Singh, J. Therm. Anal. Calorim. 105,(1), (2011), pp. 229-238.

[4] D. Nallamuthu, P. Selvarajan, T. H. Freeda, Physica B-Conden. Matter. 405(24),(2010), pp. 4908-4913.

[5] **S.** Suri, K.K. Bamzai, V. Singh, Ferroelectics. 423,**(**2011**),** pp. 94-104.

[6] W. Huang, D.E. Day, M.N. Rahaman. J. Amer. Ceram. Soc., 90(3), (2007), pp. 838-844.

[7] E. Banks, R/ Chianelli, F.Pintchovsky, J. Cryst. Growth, 18(2), (1973), pp. 185-190. [8] C. Duan, X. Wu, H. Chen, X. Yang, J. Zhao, Wuji Cailiao Xuebao/J. Inorg. Mater., 20(5), (2005), pp. 1043-1048.

[9] C. Kato, K. Fujita, K. Matsuda, Nippon Kagaku Kaishi / Chem. Soc. Japan Chem. Ind. Chem. J., (7), (1996), pp. 636-637.

[10] T. Nishino, N. Ishizawa, Nippon Seramikkusu Kyokai Gakujutsu Ronbunshi, J. Ceram. Soc. Japan, 108(6), (2000), pp. 575-580.

[11] P. Parhi, A.R. Ray, A.Ramanan, J. Amer. Ceram. Soc., 90(4), (2007), pp. 1237-1242.

[12] K.C. Hebber, S.M. Dharma Prakash, P. Mohan Rao, Bull Mater Sci. 14,(1991), pp.1219–23.

[13] D.Y. Pan, D.R. Yuan, H.Q. Sun, S.Y. Guo, X.Q. Wang, X.L. Duan, C.N. Luan, Z.F. Li. Cryst. Res. Technol.,41,(2006), pp. 236–8.

[14] S. K. Arora, T. R. Trivedi, A.T. Oza, V.A.Patel. Acta Materialia, 49(11), (2001), pp. 2103-2107.

[15] S.K. Arora, T.R. Trivedi, V.A. Patel. Scrip. Mater., 47(10), (2002), pp. 643-647.

[16] T. BenChaabane, L. Smiri, A. Bulou, Solid State Sci., 6(2), (2004), pp. 197-204.

[17] F. Wang, G. Xu, Z. Zhang, Mater. Lett., 59(7), (2005), pp. 808-812.

[18] H.A. Höppe, M. Daub, O. Oeckler, Solid State Sci., 1(8),(2009), pp. 1484-1488.

[19] G.Herzberg, Molekülspektren und Molekülstruktur. I. Zweiatomige Moleküle, Steinkopff, Dresden, 1939.

[20] N. B. Colthup, L.H. Daly, S.E. Wiberley, Introduction to Infrared and Raman Spectroscopy Academic Press, New York 1964.

[21] B. D.Cullity, Elements of X-ray Diffraction, second ed., Addison-Wesley, Massachusetts,1977.